diversity

MDPI

Article

Dynamics of Phyto- and Bacterioplankton in Southern Baikal and Irkutsk Reservoir During the Open Water Period of 2023 According to Metabarcoding Data

Yuri Galachyants *, Darya Petrova *, Artem Marchenkov, Maria Nalimova and Yelena Likhoshway

Limnological Institute, Siberian Branch of the Russian Academy of Sciences, 3 Ulan-Batorskaya Street, Irkutsk 664033, Russia; marchenkov.am@gmail.com (A.M.); yel@lin.irk.ru (Y.L.)

* Correspondence: yuri.galachyants@lin.irk.ru (Y.G.); daryapetr@gmail.com (D.P.)

Abstract: Artificial reservoirs formed by hydroelectric dams are young ecosystems requiring water quality monitoring, as they often serve local populations. Traditionally, this is performed through hydrochemical and sanitary assessments, alongside phytoplankton composition analysis. This study aimed to assess the seasonal dynamics of microbial communities—both bacterioplankton and microeukaryotes including phytoplankton—in the Irkutsk Reservoir (IR), which is fed by the cold oligotrophic waters of Southern Baikal (SB). Using parallel metabarcoding of 16S and 18S rRNA gene fragments, we analyzed community composition during the open-water season and evaluated the ecological connectivity between these two freshwater systems. We demonstrated that seasonal changes in microeukaryotic communities were closely linked between SB and IR, with the greatest divergence observed in early summer and progressive convergence by autumn. Metabarcoding confirmed microscopy-based observations while providing higher taxonomic resolution and detecting otherwise overlooked groups. Bacterioplankton communities also exhibited seasonal variation and were shaped by environmental gradients and reservoir characteristics. Cyanobacteria peaked in SB in late summer but did not dominate communities, unlike in mesotrophic lowland reservoirs. These findings demonstrate the value of metabarcoding for freshwater monitoring and provide new insights into microbial community dynamics in river–reservoir systems influenced by oligotrophic lake inflow.

Keywords: metabarcoding; 16S and 18S rRNA gene fragments; oligotrophic freshwater ecosystems; lake–river transition; seasonal dynamics

check for updates

Academic Editor: Stephan Koblmüller

Received: 11 March 2025
Revised: 17 May 2025
Accepted: 20 May 2025
Published: 22 May 2025

Citation: Galachyants, Y.; Petrova, D.; Marchenkov, A.; Nalimova, M.; Likhoshway, Y. Dynamics of Phyto- and Bacterioplankton in Southern Baikal and Irkutsk Reservoir During the Open Water Period of 2023 According to Metabarcoding Data. *Diversity* **2025**, *17*, 369. https://doi.org/10.3390/d17060369

Copyright: © 2025 by the authors. Licensee MDPI, Basel, Switzerland. This article is an open access article distributed under the terms and conditions of the Creative Commons Attribution (CC BY) license (https://creativecommons.org/licenses/by/4.0/).

1. Introduction

Phytoplankton is a key component of freshwater ecosystems, providing primary production and forming the base of food chains. Data on phytoplankton structure and abundance serve as indicators of water quality and ecosystem health. Traditionally, such information has been obtained through microscopy. However, in recent years, the application of metabarcoding of marker genes, primarily 18S rRNA gene fragments, has expanded the understanding of microeukaryotic aquatic community structure.

This method allows scalable and cost-effective profiling of eukaryotic planktonic communities, including freshwater protists such as dinoflagellates, ciliates, and cryptophytes, providing a more comprehensive picture of plankton structure and dynamics [1,2]. It also enables the identification of environmental factors affecting community composition [3], including anthropogenic influences [2,4]. The technical aspects of metabarcoding for characterizing microeukaryotic aquatic communities are constantly evolving and improving [5–9].

Metabarcoding of the 16S rRNA gene not only reveals the cyanobacterial component of communities but also identifies eubacteria and archaea. This method helps determine the structure of bacterioplankton and assess lake eutrophication levels [10], and it is used to identify pathogenic bacteria in drinking water [11].

One of the major advantages of metabarcoding is its ability to simultaneously analyze microeukaryotic and bacterioplankton communities, providing a more comprehensive understanding of their structure and ecosystem function. The combined application of 18S and 16S rRNA gene metabarcoding allows for a more complete characterization of microscopic organism communities and the study of their dynamics. Recently, the seasonal dynamics of microeukaryotes and bacteria in Southern Baikal were investigated using this approach [12].

It is important to note, however, that parallel 16S/18S metabarcoding provides a split view of microbial communities—separately resolving prokaryotic and microeukaryotic components—rather than a fully integrated picture. Comprehensive community profiling, including detection of viruses and functional gene content, can only be achieved via shotgun metagenomics. This approach offers significant advantages such as strain-level resolution, detection of non-rRNA genes, and simultaneous coverage of all microbial domains. However, it is also much more resource-intensive, requiring deeper sequencing efforts, higher costs, and more complex data analysis. Its application to freshwater monitoring is often constrained by budget and sample throughput.

Third-generation sequencing technologies such as Oxford Nanopore and PacBio now enable long-read amplicon sequencing that can span entire rRNA operons. These methods have the potential to reduce PCR biases and improve taxonomic resolution compared with short-read methods. Nonetheless, they are still under development for ecological applications and remain more expensive per read.

Metabarcoding has proven useful for monitoring artificial reservoirs. Using 18S and 16S rRNA gene metabarcoding, researchers have characterized the diversity and transformation of freshwater protists [13] and cyanobacteria [14,15] in reservoirs of the Volga basin.

The Irkutsk Reservoir (IR) is the uppermost and oldest artificial water reservoir in the Angara cascade of reservoirs and is directly connected to the upstream oligotrophic, cold-water Lake Baikal (Figure 1). Before the construction of the Irkutsk Hydroelectric Power Station, the phytoplankton of the Angara River had a distinctly lacustrine character, reflecting the phytoplankton development in Southern Baikal [16].

During the initial flooding of the Irkutsk Reservoir in 1957 [17], due to intensive shoreline erosion and the flooding of settlements in the lower impoundment area, conditions favored the dominance of the cyanobacteria *Oscillatoria* and *Anabaena* and the golden alga *Dinobryon*. The following year (1958), cyanobacteria disappeared, and the diatom *Ulnaria acus* (*Synedra acus*) and green alga *Ankistrodesmus pseudomirabilis* (now classified as *Monoraphidium arcuatum*) dominated, but overall phytoplankton abundance was low. In the summer of 1960, the diatom *Asterionella formosa* appeared in the reservoir plankton, and by 1962, species composition had become more diverse. During the reservoir's filling period (1957–1962), phytoplankton had low species diversity, with a few dominant species and weak cyanobacterial development. This type of phytoplankton composition, characterized by a small number of dominant species, is typical of oligotrophic lakes and was inherited by the Irkutsk Reservoir from Lake Baikal [17]. During the stabilization period of the Irkutsk Reservoir (1973–1987), the number of algal species and their abundance increased [18]. The dominant complex consisted of 12 species, mostly Baikal plankton species, including 8 diatoms, 2 cryptophytes, and 1 golden algal species. Cyanobacteria were not among the dominant species [18].

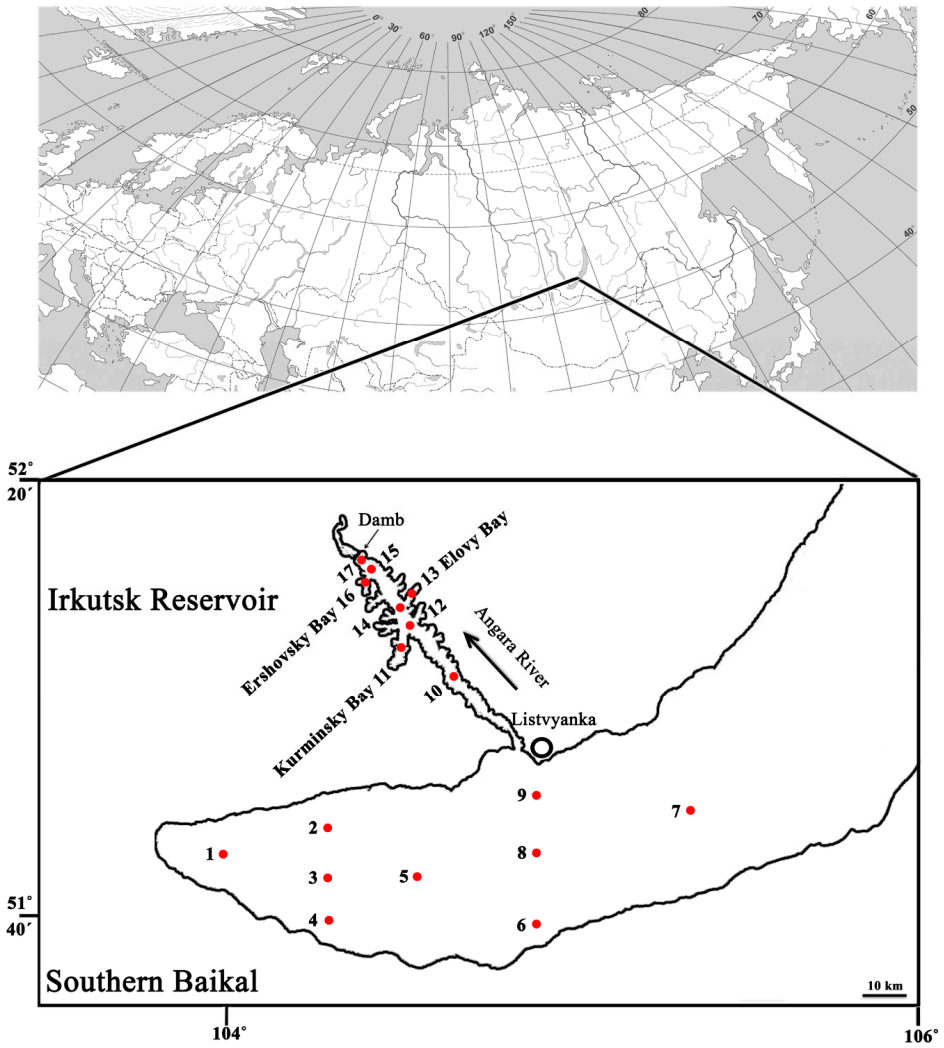


Figure 1. Schematic map of sampling points in Southern Baikal and Irkutsk Reservoir. Red dots indicate the sampling sites and their corresponding numbers. For a detailed description of sample IDs, see the column legend in Table S1.

Recent studies using optical and electron microscopy have shown that since the reservoir's creation, phytoplankton species richness has increased, and differences in its composition between SB and IR have been identified [19–21].

In this study, we examined the structure of microeukaryotic and bacterioplankton communities using metabarcoding. We used samples collected from Southern Baikal and the Irkutsk Reservoir during the open-water period (June, August, and October 2023) to create amplicon libraries and perform high-throughput sequencing (HTS) of 16S and 18S rRNA gene fragments. We then conducted a comparative analysis of community structure, identified clustering patterns, and assessed the influence of environmental parameters and ecosystem type on community structure.

We demonstrated that microeukaryotic and bacterioplankton communities undergo seasonal changes. Additionally, despite the Irkutsk Reservoir's dependence on Southern Baikal, bacterioplankton and microeukaryotic communities in SB and IR differed in early summer but became nearly identical by autumn. Furthermore, the results of microscopic data analysis [19–21] qualitatively corresponded with metabarcoding community data.

2. Materials and Methods

2.1. Sampling and Environmental Parameters

Sampling was carried out during expeditions within the framework of the Russian Science Foundation project in Southern Baikal (SB) and the Irkutsk Reservoir (IR) on 22–26 June (hydrological spring) [19], 17–20 August [20], and 15–17 October [21], 2023. Additionally, samples were collected at a station 3 km away from Listvyanka Village (51°49′033″ N 104°54′616″ E) after ice melt on 1 June, then on 16 July and 14 September 2023 (Figure 1) [21].

During sampling, temperature and pH were measured, and water transparency was determined using a Secchi disk (S, m). In the laboratory, frozen water samples were thawed at room temperature. The mineral forms of biogenic elements were determined after filtration using cellulose acetate membrane filters with 0.45 µm pores (Vladisart, Vladimir, Russia) to remove suspended matter. We carried out hydrochemical analyses of the water for its Si, PO_4^{3-}, NO_2^-, NO_3^-, and NH_4^+ content. The methods for sampling and analyzing hydrochemical parameters and the raw data on environmental factors at the sampling points were published previously [21] (Table S1).

2.2. Amplicon Library Preparation, Sequencing, Raw Data Processing, and Quality Control

To collect biomass, 10 L of a mix of equal volumes of water samples from 0.5 to 25 m depth collected at a specific site (Figure 1) was prefiltered with a 100 µm nylon mesh, and then filtered through a 0.2µm analytical track membrane (Reatrek, Russia) using an AF-142 pressure filtration unit (Vladisart, Russia), which included a compressor and a 20 L stainless steel pressure vessel. The biomass was washed off the filters into sterile TE buffer (10 mM Tris–HCl, 1 mM EDTA, pH 8.0) and stored at −80 °C until analysis. DNA was extracted using lysozyme (1 mg/mL), proteinase K, 10% SDS, and a phenol:chloroform:isoamyl alcohol mixture (25:24:1) according to the protocol based on Rush et al., 2007 [22], and described in detail in Bukin et al., 2023 [23].

Purified genomic DNA was sent to an HTS provider for amplicon library preparation and sequencing. The V3–V4 variable regions of the 16S rRNA gene were amplified with the primer pair U341F (5′-CCTACGGGRSGCAGCAG-3′) and U785R (5′-GGACTACCVGGGTATCTAAKCC-3′) [24]. The V8–V9 variable regions of the 18S rRNA gene were targeted with the primer pair V8f (5′-ATAACAGGTCTGTGATGCCCT-3′) and 1510R (5′-CCTTCYGCAGGTTCACCTAC-3′) [25]. Amplicon library preparation was performed as described in the "Illumina 16S Metagenomic Library Preparation Guide #15044223 Rev. B". Libraries were analyzed at the Smorodintsev Research Institute of Influenza (National Influenza Centre of the Russian Federation, Saint Petersburg, Russia) using an Illumina MiSeq sequencer with a Reagent Kit v3 to obtain 300 bp paired-end reads. Raw data were deposited to NCBI SRA: PRJNA1227414 and PRJNA1227401.

Analysis of sequencing data was performed using Usearch v.10 [26], Vsearch v.2.9.1 [27], and Mothur v.1.43.10 [28]. Raw reads were merged, primer sequences were truncated, and contigs were filtered by an expected error threshold of 1.0 using Usearch (option -fastq_maxee 1.0). Next, sequences were denoised using the Vsearch command "–cluster_unoise". ASVs (amplicon sequencing variants) were subjected to chimera filtering by UCHIME-denovo, followed by UCHIME-reference in Vsearch. Finally, a community composition matrix was generated by remapping merged and quality-filtered reads to a chimera-free set of ASVs with an identity threshold of 0.99 (Vsearch command "-usearch_global").

ASV sequences were taxonomically classified using the PR2 database [29] in Mothur, with the probability cutoff set to 80%. Bacterioplankton-specific ASVs were filtered to exclude unclassified, organellar, and eukaryotic sequences. Phytoplankton-specific ASVs

were further filtered by taxonomy to remove sequences of mitochondrial and chloroplast origin, as well as multicellular eukaryotic ASVs and ASVs of unknown domain taxonomical status. ASVs were then blasted against the SILVA v.138 [30] and PR2 v.5.0.0 [29] databases using blastn v.2.12.0+, and the best hits were used to associate sequences with certain environmental, taxonomical, and physiological conditions (Tables S4–S7).

Unfortunately, amplicon libraries for bacterioplankton (J14, O4, O14, O15) and for microeukaryotic communities (O1, O5) could not be obtained. The samples L6, L14, and L45 were excluded from the analysis because they were not relevant to this study (Table 1).

Table 1. One-way ANOVA (analysis of variance) computed for environmental variables and α-diversity metrics of bacterioplankton and microeukaryotic communities.

IndepVar1	IndepVar2	DepVar	ANOVA		Kruskal–Wallis	
			p_{adj}	p_{adj} Sign	p_{adj}	p_{adj} Sign
Environmental variables						
SB	Month	Si	4.27×10^{-2}	*	4.22×10^{-2}	*
IR	Month	Si	1.76×10^{-6}	***	1.69×10^{-3}	**
SB	Month	PO_4^{3-}	2.57×10^{-5}	***	2.42×10^{-3}	**
SB	Month	NO_2^-	3.60×10^{-2}	*	2.48×10^{-2}	*
IR	Month	NO_2^-	1.42×10^{-2}	*	2.48×10^{-2}	*
SB	Month	NO_3^-	3.65×10^{-6}	***	1.69×10^{-3}	**
SB	Month	NH_4^+	3.61×10^{-2}	*	2.48×10^{-2}	*
IR	Month	NH_4^+	1.52×10^{-3}	**	6.30×10^{-3}	**
SB	Month	S	3.25×10^{-3}	**	4.57×10^{-2}	*
SB	Month	pH	6.76×10^{-2}	.	2.48×10^{-2}	*
IR	Month	pH	4.75×10^{-4}	***	5.49×10^{-3}	**
SB	Month	Temp	1.94×10^{-5}	***	1.04×10^{-3}	**
IR	Month	Temp	1.76×10^{-6}	***	2.79×10^{-3}	**
SB	Month	abundance	2.56×10^{-1}		7.37×10^{-2}	.
IR	Month	abundance	4.15×10^{-5}	***	3.62×10^{-3}	**
SB	Month	biomass	2.21×10^{-2}	*	2.79×10^{-3}	**
IR	Month	biomass	1.65×10^{-4}	***	2.77×10^{-3}	**
Alpha-diversity of bacterial communities						
SB	Month	ACE	8.89×10^{-3}	**	1.87×10^{-2}	*
Alpha-diversity of microeukaryotic communities						
SB	Month	Observed	3.14×10^{-2}	*	2.58×10^{-2}	*
SB	Month	ACE	1.11×10^{-2}	*	1.47×10^{-2}	*
SB	Month	Shannon	4.75×10^{-3}	**	1.20×10^{-2}	*
IR	Month	Shannon	6.06×10^{-1}		2.80×10^{-2}	*
SB	Month	Simpson	1.89×10^{-2}	*	2.15×10^{-2}	*
IR	Month	Simpson	8.88×10^{-1}		2.57×10^{-2}	*
SB	Month	InvSimpson	8.65×10^{-3}	**	2.15×10^{-2}	*
IR	Month	InvSimpson	4.75×10^{-3}	**	2.57×10^{-2}	*

Column legend: IndepVar1/IndepVar2—independent variables used to divide the dataset into subgroups: types are SB or IR; months are Jun/Jul, Aug, and Sep/Oct | Dep—tested dependent variable | ANOVA/Kruskal–Wallis p-values: p_{adj}—FDR-adjusted (false-discovery rate) p-value | p_{adj} sign—the adjusted p-value significance code: *** ≤ 0.001; $0.001 \leq$ ** ≤ 0.01; $0.01 \leq$ * ≤ 0.05; $0.05 \leq$. ≤ 0.1.

2.3. Bioinformatics, Statistical Analyses, and Data Visualization

Exploratory analyses of community composition were performed using vegan v.2.5-6 [31] and phyloseq [32]. For exploratory analyses, ASVs with a read count above 50 were selected to create a count matrix. ASV counts were transformed using the Hellinger procedure and subjected to transformation-based principal component analysis (tb-PCA). Linear regression of explanatory variables was performed using the envfit function of the

vegan package, followed by adjustment of permutation-based regression *p*-values using the FDR procedure. Environmental factors with an adjusted *p*-value below 0.05 were plotted on the ordination plane.

For constrained ordination, eJ9, Jl9, and S9 profiles were excluded since these samples lacked environmental variable data for RDA (redundancy analysis) [21] (Table S1). Both forward selection and backward elimination approaches were tested to produce RDA models.

The top 100 most abundant ASVs from the 16S and 18S datasets were visualized using the R package pheatmap [33]. ASV counts were transformed using $\log_2(x + 1)$. The R package apcluster [34] was used for β-diversity cluster analysis. The pairwise distance matrix was computed using the Bray–Curtis similarity index, and clusters were generated using affinity propagation, followed by exemplar-based agglomerative clustering.

One-way ANOVA and Kruskal–Wallis statistical tests were used to examine the impact of independent factors on continuous environmental variables and alpha-diversity metrics associated with bacterioplankton and microeukaryotic community profiles. The obtained *p*-values were adjusted using FDR procedure.

3. Results

3.1. Difference of Environmental Factors and General Diversity Metrics Observed for Bacterioplankton and Microeukaryotic Communities

ANOVA of environmental factors and alpha-diversity (Tables S1–S3) revealed significant differences in their values depending either on the sampling location (SB/IR) or the sampling time (Table 1). In particular, significant differences were observed in Si concentration and water temperature, which peaked in August (Figure S1(A1,A8)). Phosphate and nitrate anion concentrations and water transparency were higher in SB in June–July (Figure S1(A2,A4,A6)). Total phytoplankton abundance and biomass showed maximal values in IR in June–July.

The analyzed amplicons provided sufficient coverage after ASV generation and taxonomic filtering (Table S1). The alpha-diversity of bacterioplankton differed significantly for SB communities in the ACE richness index between June–July and August–October (Figure S1(B2)). For microeukaryotes, there were significant differences in all alpha-diversity metrics. Richness and ACE had a peak in SB in August (Figure S1(C1,C2)). Shannon, Simpson, and Inverse Simpson metrics were slightly lower in June–July than in August–October.

For exploratory analysis, occurrence tables containing 1165 bacterioplankton ASVs (Tables S4 and S5) and 1081 microeukaryotic ASVs (Tables S6 and S7) were used.

3.2. Taxonomic Composition and Dynamics of Bacterioplankton Communities

Among bacterioplankton, the most abundant ASVs belonged to the classes Bacteroidia, Acidimicrobiia, Actinobacteria, Cyanophyceae, Gammaproteobacteria, Alphaproteobacteria, Verrucomicrobiae, Ignavibacteria, Nitrososphaeria, Chloroflexia, Planctomycetacia, Deltaproteobacteria, and Nitrososphaeria (Figure 2).

Bacteroidia, Acidimicrobiia, and Actinobacteria were dominant in both SB and IR ecosystems. The SB bacterioplankton communities exhibited greater diversity among minor bacterial classes, particularly in August–September and October, compared with IR. Gammaproteobacteria and Alphaproteobacteria were also well represented, maintaining relatively stable proportions across both ecosystems.

In terms of seasonal variation, in June–July, communities were relatively balanced, with Bacteroidia, Acidimicrobia, and Actinobacteria dominating, followed by Actinobacteria, Gammaproteobacteria, and Alphaproteobacteria. In August–September, the abundance

of Cyanophyceae, Planctomycetacia, and Verrucomicrobiae increased, particularly in SB. In October, Bacteroidia dominance became more pronounced, while the abundance of minor classes declined.

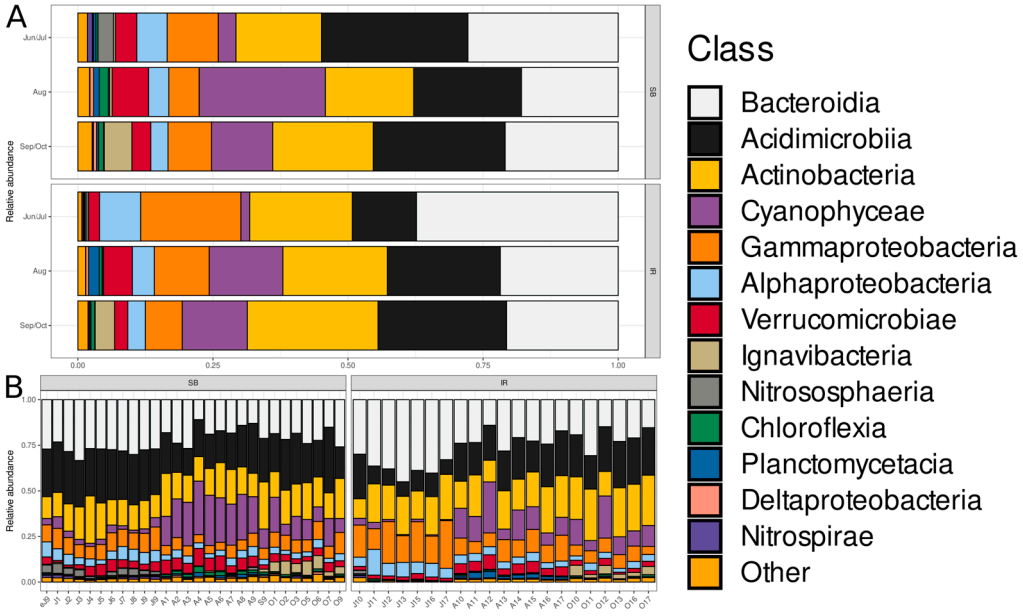


Figure 2. Hellinger-transformed relative abundances of the top 13 bacterioplankton classes in SB and IR communities. (**A**) Average abundance in communities grouped by "Type" and "Month" factor variables. (**B**) Individual community profiles grouped by "Type" factor variable. The bar stacks are horizontally sorted by month and sampling site. Taxa presented in the color legend are sorted by relative abundance in decreasing order, except for the last category, "Other". The order of classes in each bar is the same as in the color legend.

Considering the class-specific trends, Bacteroidia was consistently dominant across all seasons and ecosystems. Acidimicrobia maintained moderate proportions year-round but showed considerably lower abundance in June–July in IR compared with SB. Gammaproteobacteria fluctuated slightly but remained a key component of community structure, with higher abundance in June–July in IR compared with SB. Alphaproteobacteria remained stable but exhibited minor seasonal variations. Planctomycetacia, Verrucomicrobiae, and Cyanophyceae were more prominent in August–September, particularly in SB. Other minor classes, such as Deltaproteobacteria, Nitrospirae, and Chloroflexia, were present in small proportions.

3.3. Taxonomic Composition and Dynamics of Microeukaryotic Communities

The most abundant microeukaryotic classes identified were: Chrysophyceae, Spirotrichea, unidentified fungi, Cryptophyceae, Mediophyceae (diatoms), unidentified Alveolata, Coscinodiscophyceae (diatoms), Dinophyceae, Prymnesiophyceae, Oligohymenophorea, Trebouxiophyceae, TelonemiaXX, Chlorophyceae, unidentified Opisthokonta, Novel-clade-10-12 (Cercozoa), Bacillariophyceae (diatoms), and unidentified Cercozoa (Figure 3).

The dominant groups varied significantly between SB and IR, especially in June–July and August. Mediophyceae and Alveolata were dominant in IR, particularly in August, but were much less represented in SB. Chrysophyceae and Spirotrichea were consistently present in both ecosystems. In terms of seasonal variation, in June–July, SB microeukaryotic communities had high proportions of Fungi and Chrysophyceae, while IR communities had higher proportions of Coscinodiscophyceae, Dinophyceae, and Prymnesiophyceae. In August, Mediophyceae and Alveolata became dominant in IR, while SB exhibited a

more evenly distributed community including Oligohymenophorea, Trebouxiophyceae, and Telonemia. In September–October, both SB and IR showed increased proportions of Spirotrichea and Alveolata, along with a significant presence of Chrysophyceae in IR. Considering the class-specific trends, Chrysophyceae was present in nearly all seasons except in IR in August. Spirotrichea showed stable representation across seasons but increased in September–October. Mediophyceae dominated IR in August, reflecting a strong seasonal shift. Alveolata followed a similar trend, becoming more dominant in August and September–October. Fungi were particularly abundant in SB during June–July. Coscinodiscophyceae and Dinophyceae were well represented in IR in June–July but declined later. Bacillariophyceae appeared in moderate proportions in June–July but declined afterwards. Minor groups, such as Trebouxiophyceae, Oligohymenophorea, and Telonemia, were more prominent in SB than in IR, particularly in August.

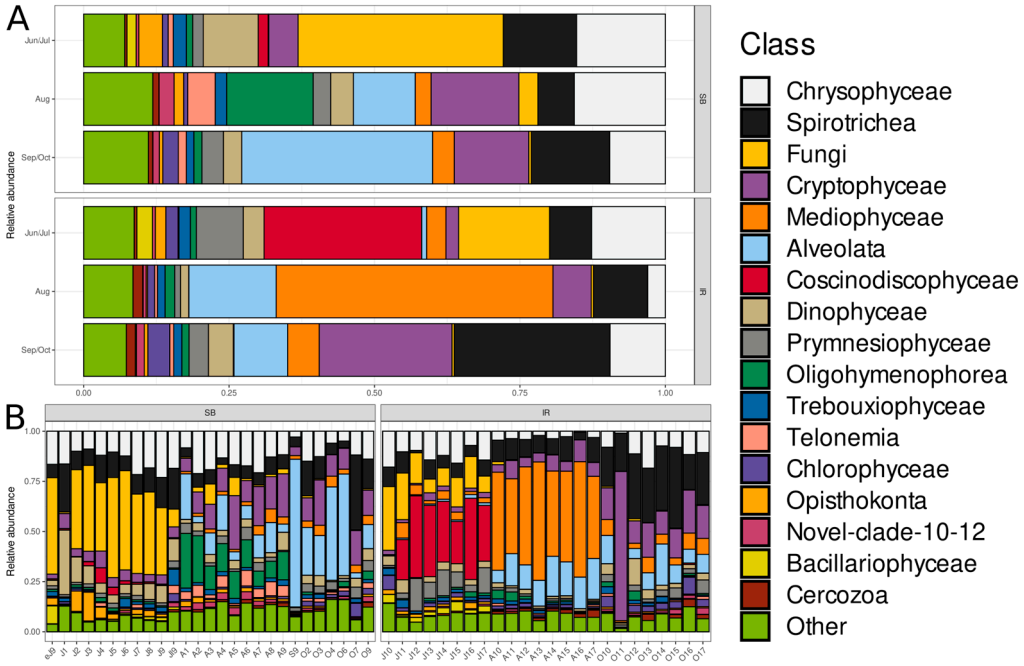


Figure 3. Hellinger-transformed relative abundances of the top 17 microeukaryotic classes in SB and IR communities. (**A**) Average abundance in communities grouped by "Type" and "Month" factor variables. (**B**) Individual community profiles grouped by "Type" factor variable. The bar stacks are horizontally sorted by month and sampling site. Taxa presented in the color legend are sorted by relative abundance in decreasing order, except for the last category, "Other". The order of classes in each bar is the same as in the color legend.

3.4. Ordination and Clustering of the Community Profiles

Unconstrained ordination (Figure 4A) revealed three distinct bacterioplankton community groups. A cluster of June communities from SB and IR was identified, as well as a more dispersed group of the remaining communities. For microeukaryotic communities (Figure 4B), clusters included (i) a group of June–July profiles from SB and IR, (ii) a cluster of August IR profiles, and (iii) a cluster of August–October profiles from SB and IR.

Interestingly, the early June and July samples collected at site 9 (3 km from Listvyanka) grouped with the June SB communities in both bacterioplankton and microeukaryotic community ordination. Another notable observation was that the bacterioplankton community at site J10 (Burduguz) occupied an intermediate position between the centroids of June–July SB and IR communities, whereas the microeukaryotic community profile of the same sample clustered within the centroid of June–July SB communities.

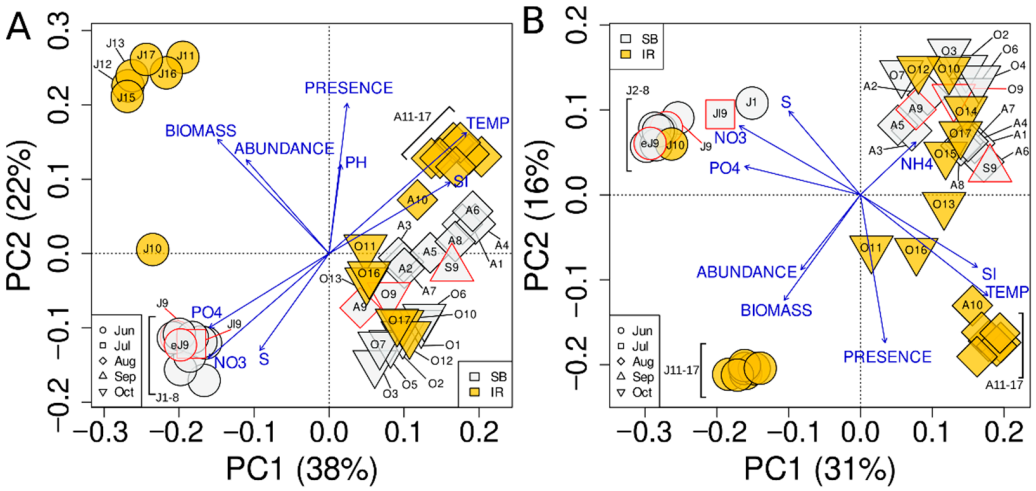


Figure 4. Unconstrained ordination of bacterioplankton (**A**) and microeukaryotic (**B**) community profiles using tb-PCA. Shape of the points represents the month of sampling, and color denotes the sampling site type: Lake Baikal or the Irkutsk Reservoir. Points outlined in red are communities sampled monthly at L3 (Listvyanka, 3 km from the shore).

Direct gradient analysis using RDA (Figure 5) produced an ordination pattern similar to PCA (Figure 4). The main difference between PCA and RDA was that August and October microeukaryotic profiles sampled in SB were more clearly separated in the RDA plot (Figure 5B) compared with PCA (Figure 4B).

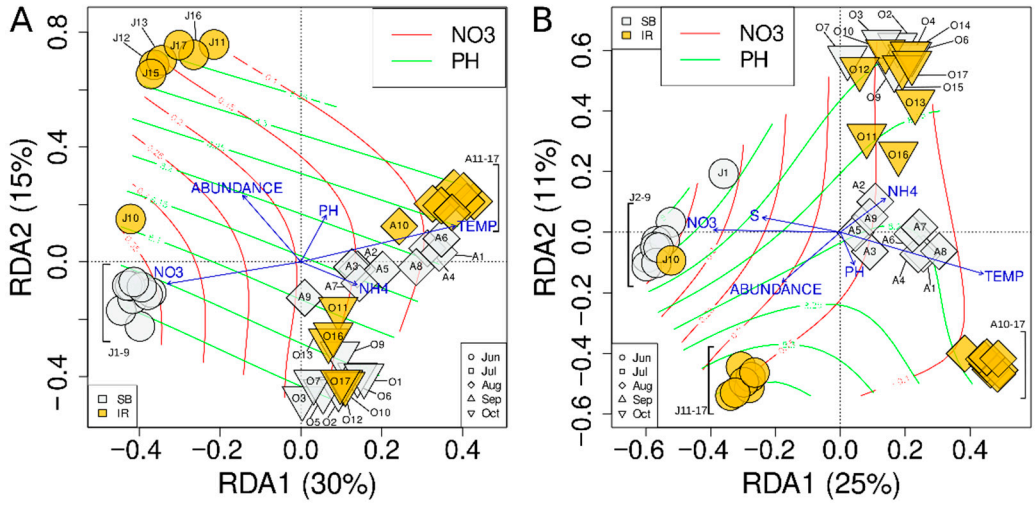


Figure 5. Constrained ordination of the bacterioplankton (**A**) and microeukaryotic (**B**) community profiles, excluding eJ9, JI9, and S9, using tb-RDA. Color and shape of the points as in Figure 4B. Red and green isolines show the gradient of nitrate anion concentration and pH, respectively.

The RDA model for bacterioplankton, inferred using both forward selection and backward elimination approaches, included nitrate anion and ammonium cation concentrations, water temperature, pH, and phytoplankton abundance as explanatory variables (Figure 5A). The total variation explained by the full model was 52.1%, while the adjusted R^2 of the final model (i.e., its explanatory power) was 50.5%.

Similarly, the RDA model for microeukaryotic communities included the same explanatory variables, plus water transparency measured by a Secchi disk (Figure 5B). The total variation explained by the full model was 45.9%, and the adjusted R^2 was 45%.

Clustering analysis using the affinity propagation method (Figure 6) showed that both bacterioplankton and microeukaryotic communities were grouped into (i) a cluster of

June–July profiles, which further divided into separate SB and IR communities, (ii) and a cluster of August–October communities. In this second group, August bacterioplankton and microeukaryotic communities were separated into SB and IR subclusters, whereas in September–October, such separation was observed only for microeukaryotic communities. Overall, these results were consistent with the findings from unconstrained ordination (Figures 4 and 5).

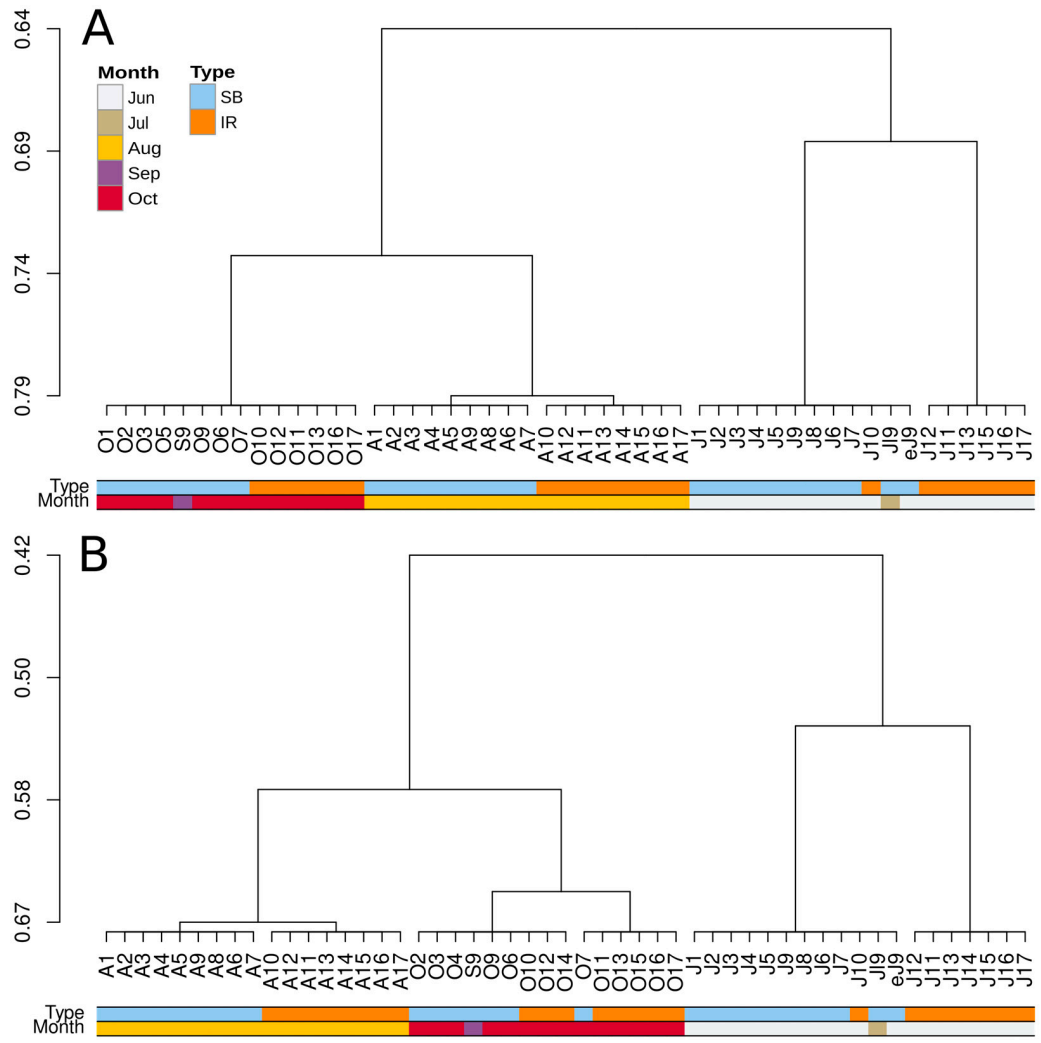


Figure 6. Cluster analysis of the bacterioplankton (**A**) and microeukaryotic (**B**) community profiles using affinity propagation.

3.5. Bacterioplankton ASV Sequence Matches Against SSU rRNA Reference Databases in Terms of Environmental, Ecological, and Geographical Context

The bacterial ASVs identified in SB and IR matched nucleotide sequences of bacteria from a wide range of aquatic environments (Tables S3, S4 and S7). The most abundant bacterioplankton ASVs showed strong sequence similarities (Table S8) with organisms found in (i) oligotrophic lakes (e.g., Crater Lake, USA, and Lake Zurich, Switzerland), which are characterized by low nutrient concentrations and high oxygen levels; (ii) mesotrophic lakes (e.g., Lake Stechlin, Germany), which have moderate nutrient levels that support diverse microbial communities; (iii) high-altitude and polar lakes (e.g., Tibetan Plateau lakes and Arctic freshwater systems), highlighting their adaptability to cold and low-nutrient conditions; and (iv) and glacial and subglacial environments (e.g., glacial meltwaters and subglacial sediments), indicating resilience to extreme conditions.

The identified bacteria exhibited a cosmopolitan distribution, with close relatives detected in freshwater ecosystems across multiple continents, including North America, Europe, Asia, and the polar regions of the Arctic and Antarctic. The predominant bacterial groups (Figures 2 and 7) included (i) Actinobacteria, notably the acI lineage, common in the freshwater environments; (ii) Proteobacteria, particularly Betaproteobacteria and Pelagibacterales, which play key roles in nutrient cycling; (iii) Bacteroidetes, such as Flavobacteria and Cytophagales, involved in organic matter degradation; (iv) Cyanobacteria, especially genera like *Synechococcus* and *Cyanobium gracile*, which are likely primary producers; (v) and Verrucomicrobia, contributing to polysaccharide degradation.

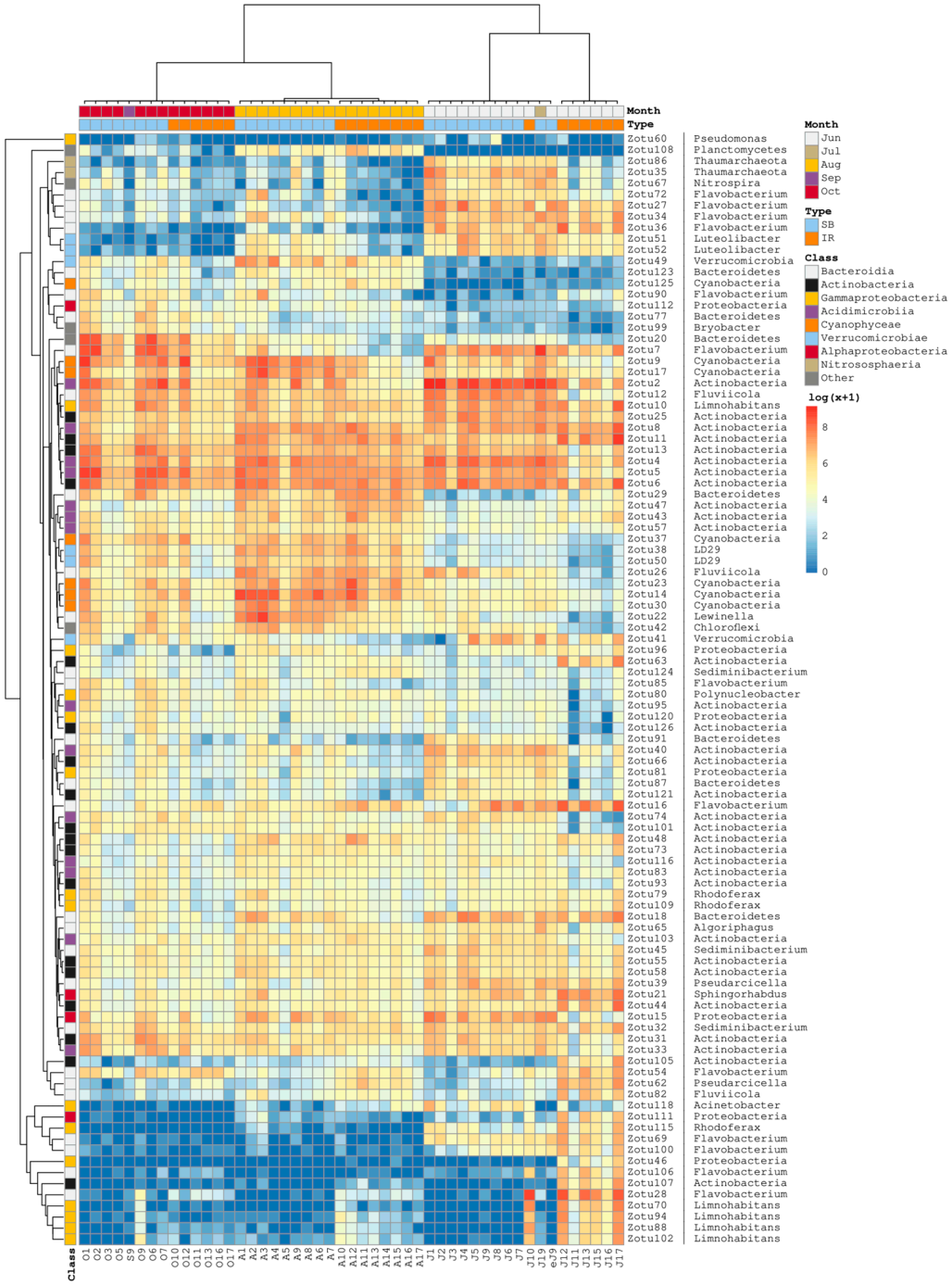


Figure 7. Heatmap of the bacterioplankton community profiles generated with a set of 100 most abundant ASVs. The order of communities (columns) is the same as in Figure 3A. UPGMA-assisted

clustering of the Bray–Curtis pairwise distance matrices was used to produce the ASV-wise clustering tree. Color annotations above the heatmap describe the spatial and temporal categories of communities. Color annotations on the left denote the ASV taxonomic affiliation at the class level. The genus or higher-level taxonomic classification is provided to the right of each ASV identifier.

3.6. Microeukaryotic ASV Sequence Matches Against SSU rRNA Reference Databases in Terms of Environmental, Ecological, and Geographical Context

The microeukaryotic ASVs from SB and IR matched nucleotide sequences of free-living unicellular eukaryotes associated with various freshwater habitats (Tables S6, S7 and S9). The most abundant microeukaryotic ASVs showed strong sequence similarities (Table S9) with organisms found in (i) planktonic communities dominant in both oligotrophic and mesotrophic lakes, indicating adaptability to different nutrient levels; (ii) meromictic lakes (e.g., Lake Pavin, France), suggesting specialization in stratified water columns; and (iii) hypolimnetic zones (deep-water adapted species), reflecting tolerance to low-light and low-oxygen conditions.

The microeukaryotic taxa exhibited a broad geographical distribution, including North America, Europe, Asia, and lakes in Arctic and Antarctic regions. The taxonomic composition of SB and IR communities was characterized by the abundance of (i) diatoms (*Aulacoseira*, *Stephanodiscus*, and *Thalassiosira*), responsible for primary production and silica cycling; (ii) Cryptophytes (e.g., *Cryptomonas curvata*), known for mixotrophic capabilities; (iii) Ciliates (e.g., *Vorticella*, *Carchesium*, and *Meseres*), playing a role in microbial predation; (iv) Chrysophytes (e.g., *Chromulina* and *Spumella*), contributing to primary production and carbon cycling microbial predation; (v) and fungal zooflagellates (e.g., *Paraphysomonas* and *Telonema*), involved in organic matter decomposition.

3.7. Dynamics of Cyanobacterial Abundance

As noted earlier, the most intense cyanobacterial development was observed in August–September in SB (Figure 2). The seven most abundant cyanobacterial ASVs, presented in the heatmap (Figure 7)—Zotu9, Zotu14, Zotu17, Zotu23, Zotu30, Zotu37, and Zotu125—belonged to the genus *Cyanobium* (*Synechococcus*) and shared 96–97% sequence similarity with SSU rRNA reference sequences in the SILVA and PR2 databases (Tables S3, S4 and S7). Zotu9 and Zotu17 were relatively abundant across all SB and IR profiles and peaked in August. Zotu14, Zotu23, Zotu30, Zotu37, and Zotu125 also peaked in August communities but showed lower abundance at the beginning and end of summer. In addition to the highly abundant *Cyanobium*-specific ASVs, some cyanobacterial ASVs were identified that matched reference SSU rRNA sequences from the genera *Pseudanabaena*, *Aphanizomenon*, and *Dolichospermum* (Tables S3 and S4).

3.8. Dynamics of Diatom Abundance Across Different Classes

At the beginning of summer, the IR communities exhibited high ASV abundance from the class Coscinodiscophyceae (Figure 3). All these ASVs were assigned to the genus *Aulacoseira* (Tables S6, S7 and S9). The abundance variation of the most numerous ASV, Zotu3, closely followed the overall dynamics of Coscinodiscophyceae abundance (Figure 8).

BLAST analysis of the most abundant Mediophyceae ASVs (family Thalassiosirales) revealed exact or nearly exact matches with diatom sequences from the following genera: Zotu5 (*Stephanodiscus*), Zotu14 (*Thalassiosira*), Zotu29 (*Discostella*), Zotu44 (*Stephanodiscus*), Zotu67, and Zotu73 (*Detonula*). Importantly, seasonal and spatial variations in the abundance of these two ASV groups differed (Figure 8): (i) Zotu5 and Zotu29 had similar occurrence patterns, with increased abundance in June, July, and August in IR. They were also present in August SB communities and at lower levels in both SB and IR in October; (ii) Zotu14 peaked in IR in August and was found in smaller quantities in other SB and IR

communities later in summer. However, its abundance was close to zero at the beginning of summer; (iii) Zotu44 was mainly observed in the second half of summer, with higher abundance in SB communities; and (iv) Zotu67 and Zotu73 were abundant in IR communities in August but were poorly represented or absent in other profiles.

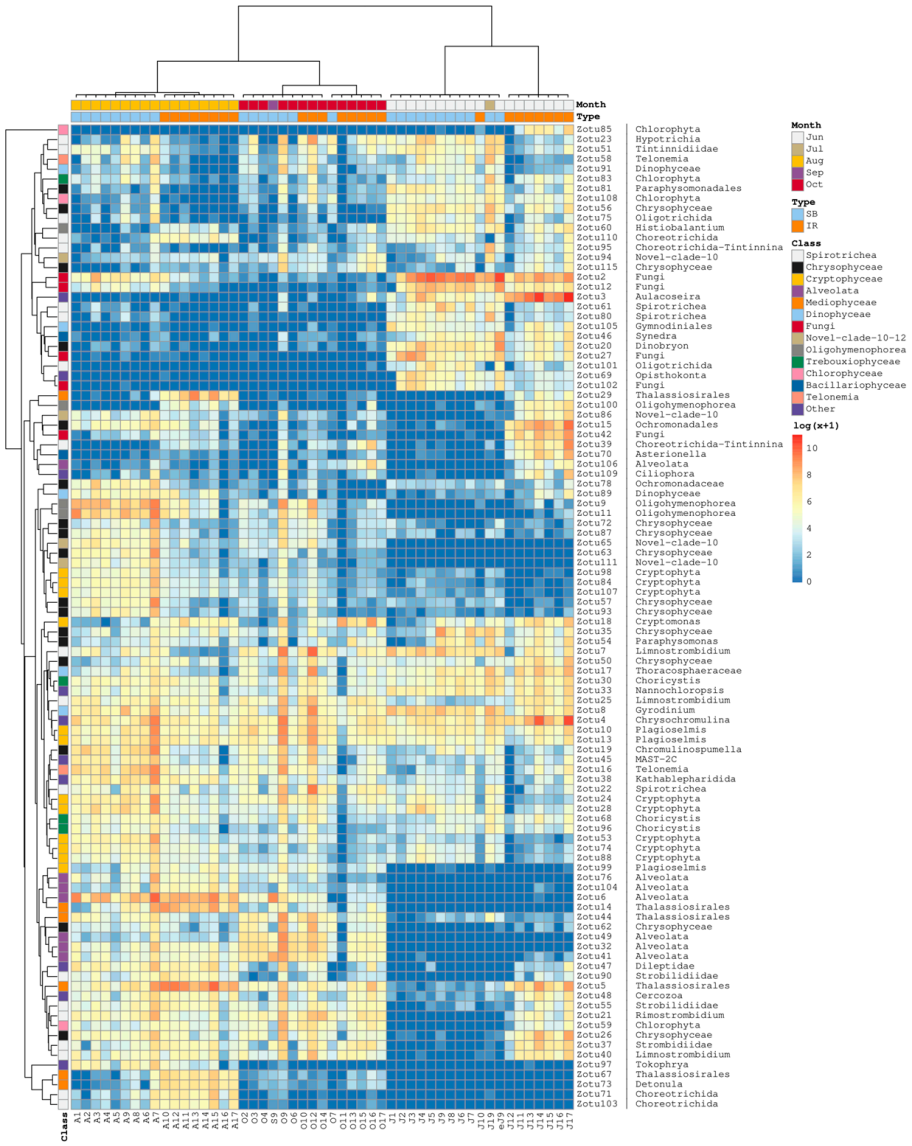


Figure 8. Heatmap of the microeukaryotic community profiles generated with a set of 100 most abundant ASVs. The order of communities (columns) is the same as in Figure 3B. UPGMA-assisted clustering of the Bray–Curtis pairwise distance matrices was used to produce the ASV-wise clustering tree. Color annotations above the heatmap describe the spatial and temporal categories of communities. Color annotations on the left denote the ASV taxonomic affiliation at the class level. The genus or higher-level taxonomic classification is provided to the right of each ASV identifier.

Two Bacillariophyceae-specific ASVs were among the top 100 most abundant: Zotu46 (*Ulnaria*) and Zotu70 (*Asterionella*). The abundance of Zotu46 peaked in June–July in both SB and IR, whereas Zotu70 was most abundant in IR in June and was detected in smaller numbers in IR communities later in summer.

Overall, the trends in Bacillariophyceae-specific ASV dynamics (Figure 8) were consistent with the overall representation of Bacillariophyceae sequences at the level of class (Figure 3).

4. Discussion

Compared with microscopy, metabarcoding detects a broader range of microeukaryotic community members. At higher taxonomic levels, the assessment of diversity and taxon abundance is comparable [35]. Our results support this statement. For instance, when analyzing the same communities using microscopy [21], similar patterns of dominant phytoplankton groups were observed.

Metabarcoding results suggest that microscopy underestimates the diversity of many microeukaryotic groups, such as picophytoplankton and flagellates with mixotrophic potential [36], which are crucial components of aquatic communities. In this study, we detected cryptophyte and chrysophyte flagellates, which is mainly consistent with the high abundance of chrysophytes observed via scanning electron microscopy of silica-scaled chrysophytes [37], though microscopic methods are more labor-intensive compared with metabarcoding.

Compared with microscopy, metabarcoding allows for faster community characterization with lower labor costs [35]. Illumina MiSeq or other HTS platforms are believed to be employed for biomonitoring and especially for real-time systems monitoring to detect target microeukaryotic groups, such as diatoms [38]. Our data confirm that key diatom groups were consistently detected in microeukaryotic community profiles from SB and IR. For example, according to microscopy data, *Aulacoseira islandica* exhibited a peak in IR communities in June–July. A similar trend was observed in the metabarcoding data (Figures 3 and 8). Thus, it can be stated with high confidence that the microeukaryotic ASV Zotu3 corresponds to a fragment of *A. islandica* SSU rRNA.

However, in most cases, ASV sequences cannot be unambiguously linked to specific species for abundance analysis. To make this systematically possible, at least two conditions must be met: (i) the availability of a reference database containing full-length nucleotide sequences of the ribosomal locus for the target microbial species and (ii) the use of modern HTS technologies capable of producing longer ASV sequences [7].

To our knowledge, there are very few published studies investigating microbial communities in freshwater systems where a large, oligotrophic lake flows into a downstream artificial reservoir. The Irkutsk Reservoir is uniquely influenced by cold, nutrient-poor waters from Lake Baikal, making it ecologically distinct from typical lowland or mesotrophic reservoirs. While direct analogues are limited, we compared our findings with metabarcoding-based studies from the Kuibyshev Reservoir [13–15] to highlight methodological parallels and the value of high-throughput sequencing for assessing seasonal microbial dynamics in artificial systems. Unlike Irkutsk, the Kuibyshev Reservoir plankton communities reflect more productive and warmer conditions. Although the ecological contexts differ, both studies applied comparable sequencing techniques, allowing us to contrast microbial community structures and the dominance of key taxonomic groups such as cyanobacteria and phytoplankton microeukaryotes. Similar studies in other cold, oligotrophic-to-mesotrophic transition zones, such as Arctic lakes with downstream glacial-fed basins, remain scarce. Therefore, our results contribute new insights into how microbial communities respond in such atypical river–reservoir systems and may serve as a reference point for future studies in similar cold-inflow artificial environments.

When metabarcoding was used to analyze plankton in the Kuibyshev Reservoir, located on the Volga River in a lowland region, 1150 OTUs (operational taxonomic units) of protists were identified. The dominant stramenopile groups were, in descending order, Chrysophyceae, Opalozoa, Diatomea, and Oomycetes (Peronosporomycetes). In terms of the number of nucleotide sequences, Alveolata—primarily Ciliata—was dominant. In our study, a total of 1081 microeukaryotic ASVs were identified, and their seasonal and spatial dynamics were characterized (Figure 3).

In August, IR experienced a strong shift toward Mediophyceae and Alveolata dominance, whereas SB maintained a more diverse and evenly distributed community. In June–July, SB communities had a high proportion of fungi, while IR communities were dominated by diatoms (Coscinodiscophyceae and Dinophyceae). In September–October, IR showed increased proportions of Chrysophyceae and Spirotrichea, while SB retained high community diversity.

SB exhibited greater seasonal fluctuations in bacterioplankton community composition compared with IR. In August–September, there was the highest diversity, with increased abundance of Planctomycetacia, Verrucomicrobiae, Cyanophyceae, and other minor classes. In October and June–July, microbial communities were dominated by Bacteroidia, Acidimicrobiia, and Actinobacteria, suggesting a shift toward a more simplified community structure (Figure 2).

Previous research on the Kuibyshev Reservoir [13] has shown that cyanobacterial diversity estimates obtained through microscopy and metabarcoding are similar. The dominant complex structure identified by both methods matched well at the family and order levels. However, at the genus and species levels, as well as among minor taxa, noticeable differences were observed. According to both microscopy and metabarcoding, the "core" cyanobacterial community in the Kuibyshev Reservoir consisted of representatives of the families Aphanizomenonaceae, Prochlorococcaceae, and Microcystistaceae, with *Aphanizomenon–Dolichospermum* species complex dominating. Our data indicate that the core community in SB was primarily composed of *Cyanobium* (*Synechococcus*), which peaked in August and gradually declined toward October (Figure 2). Results also suggest that other cyanobacterial picoplankton representatives, such as *Pseudanabaena*, *Aphanizomenon*, and *Dolichospermum*, did not reach high abundances in the analyzed bacterioplankton communities.

However, the authors emphasize that the number of sequences obtained via metabarcoding does not directly correspond to either the number or the biomass of cells, and it should be considered as an independent community characteristic [13]. As noted earlier, our results support this viewpoint. In most cases, additional efforts are required to link species abundance data with OTU/ASV counts.

Previous microscopy-based studies of SB and IR communities have shown that in spring, the primary factor influencing the distribution of microeukaryotic species in SB and IR is water temperature [19]. This is obviously due to the fact that IR becomes ice-free earlier and warms up faster than SB, owing to its shallower depth. In summer communities, pH and water transparency were the most significant correlating factors [20]. A comprehensive seasonal phytoplankton analysis using microscopy revealed that the most important factors shaping community structure were nutrient concentrations, temperature, water transparency, and pH [21]. ANOVA of environmental factors and microeukaryotic alpha-diversity based on metabarcoding data (Table 1, Figure S1) confirmed and complemented previously identified patterns.

Furthermore, ordination analysis of both bacterioplankton and microeukaryotic communities showed patterns similar to those obtained through microscopy (Figures 4 and 5). Similarly, in constrained ordination of metabarcoding data, the primary explanatory variables were nutrient concentrations, temperature, water transparency, phytoplankton abundance, and pH.

The Irkutsk Reservoir plays an important role in supporting local communities, with several settlements and drinking water intakes situated along its shores. Although this study was not designed to assess specific ecosystem services or health risks, the microbial community data we present offer a valuable baseline for future monitoring. Understanding seasonal microbial dynamics—including the presence and abundance of potentially harm-

ful cyanobacteria—is essential for early warning systems and water quality management. We hope that these results can contribute to the development of ecosystem-based strategies for maintaining safe water use and protecting public health in the region.

5. Conclusions

This study demonstrates that the microbial communities of the Irkutsk Reservoir—though largely shaped by inflow from oligotrophic Lake Baikal—undergo distinct seasonal transformations, with divergence from and eventual convergence toward Baikal community profiles over time. Metabarcoding revealed fine-scale taxonomic and temporal patterns that would be difficult to capture through microscopy alone, particularly for bacterioplankton and small eukaryotes. Importantly, we were able to trace the seasonal behavior of key ecological groups, such as Cyanobacteria and diatoms, down to individual ASVs, strengthening the interpretation of microbial succession processes in regulated river-reservoir systems. These results provide a foundation for using sequence-based approaches in freshwater ecosystem monitoring and show how the influence of upstream ultraoligotrophic systems diminishes under changing seasonal and environmental pressures.

Supplementary Materials: The following supporting information can be downloaded at https://www.mdpi.com/article/10.3390/d17060369/s1, Table S1. Column legend: amp ID—amplicon ID as deposited in SRA | sample ID—ID that is used in this paper, concatenation of the month abbreviation and the sampling station number | Count of raw reads per sample: raw—after demultiplexing and merging | EC—after denoising and chimera filtering | Tax—after removal of unwanted taxa; Table S2. Alpha indices computed for bacterioplankton communities. Column legend: Sample ID and amp ID as in Table S1 | Types indicate whether the sample is from SB or IR | Months are categorized as Jun/Jul, Aug, and Sep/Oct | Reads represent the number of reads per amplicon after taxonomy filtering and removal of ASVs with fewer than 50 reads | Richness indicates the observed number of ASVs | ACE is the abundance-based coverage estimator index | Shannon, Simpson, and InvSimpson represent different diversity indices; Table S3. Alpha indices computed for microeukaryotic communities. Column legend: Same as Table S2; Table S4. Taxonomic assignment and the closest PR2 matches (≥95% identity) for bacterioplankton ASV sequences. Column legend: Readcount refers to the number of reads per ASV | Domain, Supergroup, Division, Subdivision, Class, Order, Family, Genus, and Species indicate assigned PR2 taxonomy | PR2_hits represents the best PR2 matches with identity percentages | FASTA contains the ASV nucleotide sequence; Table S5. Taxonomic assignment and closest SILVA matches (≥98% identity) for bacterioplankton ASV sequences. Column legend: Readcount refers to the number of reads per ASV | PR2_Domain, PR2_Supergroup, PR2_Division, PR2_Subdivision, PR2_Class, PR2_Order, PR2_Family, PR2_Genus, and PR2_Species provide PR2 taxonomy assignments as in Table S4 | SLV_superkingdom, SLV_phylum, SLV_class, SLV_order, SLV_family, SLV_genus, SLV_species indicate the SILVA taxonomy assignments | SLV_hits represents the best SILVA matches. Table S6. Taxonomic assignment and closest PR2 matches (≥95% identity) for microeukaryotic ASV sequences. Column legend: Same as in Table S4; Table S7. Taxonomic assignment and the closest SILVA matches (≥98% identity) for microeukaryotic ASV sequences. Column legend: Same as in Table S5; Table S8. Best PR2 and SILVA database matches for the top 50 most abundant bacterioplankton ASVs, including associated environmental, taxonomic, and geographical data; Table S9. Best PR2 and SILVA database matches for the top 50 most abundant microeukaryotic ASVs, including associated environmental, taxonomic, and geographical data. References [39–106] are cited in Supplementary Materials.

Author Contributions: Conceptualization, Y.L. and Y.G.; methodology, Y.G., D.P. and A.M.; software, Y.G.; validation, Y.G. and D.P.; formal analysis, Y.G., D.P. and M.N.; investigation, Y.G.; writing—original draft preparation, Y.G.; writing—review and editing, Y.G., D.P. and Y.L.; visualization, Y.G.; supervision, Y.L.; project administration, Y.L. All authors have read and agreed to the published version of the manuscript.

Funding: This study was supported by the Russian Science Foundation, grant number 23-14-00028 «Communities of Microeukaryotes in Angara Cascade Reservoirs», https://rscf.ru/project/23-14-00028/ (accessed on 16 May 2025).

Institutional Review Board Statement: Not applicable.

Data Availability Statement: The sequence data were submitted to the Sequence Read Archive database (https://www.ncbi.nlm.nih.gov/sra (accessed on 16 May 2025)) of the National Center for Biotechnology Information under BioProject accession numbers PRJNA1227414 and PRJNA1227401.

Acknowledgments: We thank the crew members of the research vessels *Papanin* and *Titov* (The Center for Collective Use «Research vessels Center of LIN SB RAS on Lake Baikal») for their support and cooperation during the expeditions. We are also grateful to Diana Hilkhanova and Ivan Mikhailov for their assistance in water sampling and fixation. Special thanks to the Smorodintsev Research Institute of Influenza (Saint Petersburg, Russia) and personally to Andrey Komissarov for facilitating HTS. We also acknowledge the IT department of the Limnological Institute SB RAS for providing computational infrastructure for HTS data analysis. We sincerely appreciate all the comments and suggestions of the reviewers, which helped us to improve the quality of the manuscript.

Conflicts of Interest: The authors declare no conflicts of interest.

Abbreviations

The following abbreviations are used in this manuscript:

ANOVA	analysis of variance
ASV	amplicon sequencing variant
FDR	false-discovery rate
HTS	high-throughput sequencing
IR	Irkutsk Reservoir
OTU	operational taxonomic unit
PCA	principal component analysis
RDA	redundancy analysis
SB	Southern Baikal

References

1. Banerji, A.; Bagley, M.; Elk, M.; Pilgrim, E.; Marinson, J.; Domingo, J.S. Spatial and temporal dynamics of a freshwater eukaryotic plankton community revealed via 18S rRNA gene metabarcoding. *Hydrobiologia* **2018**, *818*, 71–86. [CrossRef] [PubMed]
2. Choi, T.-J.; Malik, A.; An, H.-E.; Kim, J.-I.; Do, T.D.; Kim, C.-B. Seasonal diversity of microeukaryotes in the Han River, Korea through 18S rRNA gene metabarcoding. *Evol. Bioinform. Online* **2022**, *18*, 1–10. [CrossRef]
3. David, G.M.; Moreira, D.; Reboul, G.; Annenkova, N.V.; Galindo, L.J.; Bertolino, P.; López-Archilla, A.I.; Jardillier, L.; López-García, P. Environmental drivers of plankton protist communities along latitudinal and vertical gradients in the oldest and deepest freshwater lake. *Environ. Microbiol.* **2021**, *23*, 1436–1451. [CrossRef]
4. Lin, Y.; Wenjun, Z.W.; Zhang, X.; Zhou, X.; He, L.; Lv, J.; Zhao, Z. Environmental DNA metabarcoding revealed the impacts of anthropogenic activities on phytoplankton diversity in Dianchi Lake and its three inflow rivers. *Ecol. Evol.* **2023**, *13*, e10088. [CrossRef]
5. Santoferrara, L.; Burki, F.; Filker, S.; Logares, R.; Dunthorn, M.; Mcmanus, G.B. Perspectives from Ten Years of Protist Studies by High-Throughput Metabarcoding. *J. Eukaryot. Microbiol.* **2020**, *67*, 612–622. [CrossRef]
6. Martin, J.L.; Santi, I.; Pitta, P.; John, U.; Gypens, N. Towards quantitative metabarcoding of eukaryotic plankton: An approach to improve 18S rRNA gene copy number bias. *MBMG* **2022**, *6*, 245–259. [CrossRef]
7. Latz, M.A.C.; Grujcic, V.; Brugel, S.; Lycken, J.; Jphn, U.; Karlson, B.; Andersson, A.; Andersson, A.F. Short- and long- read metabarcoding of the eukaryotic rRNA operon: Evaluation of primers and comparison to shotgun metagenomics sequencing. *Mol. Ecol. Resour.* **2022**, *22*, 2304–2318. [CrossRef] [PubMed]
8. Pierella Karlusich, J.J.; Lombard, F.; Irisson, J.-O.; Bowler, C.; Foster, R.A. Coupling Imaging and Omics in Plankton Surveys: State-of-the-Art, Challenges, and Future Directions. *Front. Mar. Sci.* **2022**, *9*, 878803. [CrossRef]
9. Vaulot, D.; Sim, C.W.H.; Ong, D.; Teo, B.; Biwer, C.; Jamy, M.; Lopes Dos Santos, A. metaPR^2: A database of eukaryotic 18S rRNA metabarcodes with an emphasis on protists. *Mol. Ecol. Resour.* **2022**, *22*, 3188–3201. [CrossRef]

10. Skopina, M.Y.; Kuznetzova, E.V.; Tikhonenkov, D.V.; Zhang, H.; Gerasimova, E.A.; Tsvetkov, A.I.; Kosolapov, D.B. Distribution, community structure and metabolic potential of bacterioplankton in a small boreal lake: Microscopy-based survey and 16S rRNA-based DNA metabarcoding. *Limnologica* **2024**, *109*, 126213. [CrossRef]
11. Romero, P.E.; Calla-Quispe, E.; Castillo Vilcahuaman, C.; Yokoo, M.; Fuentes-Rivera, H.L.; Ramirez, J.L.; Ampuero, A.; Ibáñez, A.J.; Wong, P. From the Andes to the desert: 16S rRNA metabarcoding characterization of aquatic bacterial communities in the Rimac River, the main source of water for Lima, Peru. *PLoS ONE* **2021**, *16*, e0250401. [CrossRef] [PubMed]
12. Mikhailov, I.S.; Galachyants, Y.P.; Bukin, Y.S.; Petrova, D.P.; Bashenkhaeva, M.V.; Sakirko, M.V.; Blinov, V.V.; Titova, L.A.; Zakharova, Y.R.; Likhoshway, Y.V. Seasonal Succession and Coherence Among Bacteria and Microeukaryotes in Lake Baikal. *Microb. Ecol.* **2022**, *84*, 404–422. [CrossRef] [PubMed]
13. Umanskaya, M.V.; Gorbunov, M.Y.; Bykova, S.V.; Tarasova, N.G. Diversity and Transformation of the Freshwater Planktonic Protist Community Along the Estuarine Tributary Zone of the Large Plainland Reservoir: 18S RRNA Gene Metabarkoding. *Biol. Bull.* **2023**, *50*, 707–723. [CrossRef]
14. Umanskaya, V.; Gorbunov, M.Y.; Krasnova, Y.S.; Tarasova, N.G. Microscopic examination and 16S metabarcoding for comparative analysis of cyanobacteria community structure in a plainland reservoir. *Biosphere* **2023**, *15*, 246–260. (In Russian)
15. Umanskaya, M.V.; Gorbunov, M.Y. Phylogenetic structure of bacterioplankton in water bodies of the Kuibyshev Reservoir basin during the period of mass development of cyanobacteria. *Microbiology* **2024**, *93*, 876–890. [CrossRef]
16. Yasnitskiy, V.N. Plankton of Lake Baikal in the area of Kultuk and Slyudyanka. *Izv. ESB RGS* **1924**, *47*, 147–152. (In Russian)
17. Kozhova, O.M. Phytoplankton of the Irkutsk reservoir. In *Biology of the Irkutsk Reservoir*; Nauka: Moscow, Russia, 1964; pp. 41–114. (In Russian)
18. Vorobyova, S.S. *Phytoplankton of Angara Reservoirs*; Nauka Siberian Publishing Company of the RAS: Novosibirsk, Russia, 1995; 126p. (In Russian)
19. Firsova, A.D.; Galachyants, Y.; Bessudova, A.Y.; Titova, L.A.; Sakirko, M.V.; Marchenkov, A.M.; Hilkhanova, D.V.; Nalimova, M.A.; Buzevich, V.V.; Mikhailov, I.S.; et al. Environmental factors affecting distribution and diversity of phytoplankton in the Irkutsk Reservoir ecosystem in June 2023. *Diversity* **2023**, *15*, 1070. [CrossRef]
20. Firsova, A.; Galachyants, Y.; Bessudova, A.; Mikhailov, I.; Titova, L.; Marchenkov, A.; Hilkhanova, D.; Nalimova, M.; Buzevich, V.; Likhoshway, Y. Summer phytoplankton species composition and abundance in the southern basin of Lake Baikal and Irkutsk Reservoir. *LFWB* **2023**, *6*, 204–228. [CrossRef]
21. Firsova, A.; Galachyants, Y.; Bessudova, A.; Hilkhanova, D.; Titova, L.; Nalimova, M.; Buzevich, V.; Marchenkov, A.; Sakirko, M.; Likhoshway, Y. The Influence of Waters of Lake Baikal on the Spatiotemporal Dynamics of Phytoplankton in the Irkutsk Reservoir. *Water* **2024**, *16*, 3284. [CrossRef]
22. Rusch, D.B.; Halpern, A.L.; Sutton, G.; Heidelberg, K.B.; Williamson, S.; Yooseph, S.; Wu, D.; Eisen, J.A.; Hoffman, J.M.; Remington, K.; et al. The Sorcerer II Global Ocean Sampling Expedition: Northwest Atlantic through Eastern Tropical Pacific. *PLoS Biol.* **2007**, *5*, e77. [CrossRef]
23. Bukin, Y.S.; Mikhailov, I.S.; Petrova, D.P.; Galachyants, Y.P.; Zakharova, Y.R.; Likhoshway, Y.V. The effect of metabarcoding 18S rRNA region choice on diversity of microeukaryotes including phytoplankton. *World J. Microbiol. Biotechnol.* **2023**, *39*, 1–18. [CrossRef]
24. Baker, G.C.; Smith, J.J.; Cowan, D.A. Review and re-analysis of domain-specific 16S primers. *J. Microbiol. Methods* **2003**, *55*, 541–555. [CrossRef]
25. Bradley, I.M.; Pinto, A.J.; Guest, J.S. Design and evaluation of Illumina MiSeq-compatible, 18S rRNA gene-specific primers for improved characterization of mixed phototrophic communities. *Appl. Environ. Microbiol.* **2016**, *82*, 5878–5891. [CrossRef]
26. Edgar, R.C. Search and clustering orders of magnitude faster than BLAST. *Bioinformatics* **2010**, *26*, 2460–2461. [CrossRef] [PubMed]
27. Rognes, T.; Flouri, T.; Nichols, B.; Quince, C.; Mahe, F. VSEARCH: A versatile open source tool for metagenomics. *PeerJ* **2016**, *4*, e2584. [CrossRef]
28. Schloss, P.D.; Westcott, S.L.; Ryabin, T.; Hall, J.R.; Hartmann, M.; Hollister, E.B.; Lesniewski, R.A.; Oakley, B.B.; Parks, D.H.; Robinson, C.J. Introducing mothur: Open-source, platform-independent, community-supported software for describing and comparing microbial communities. *Appl. Environ. Microbiol.* **2009**, *75*, 7537–7541. [CrossRef] [PubMed]
29. Guillou, L.; Bachar, D.; Audic, S.; Bass, D.; Berney, C.; Bittner, L.; Boutte, C.; Burgaud, G.; de Vargas, C.; Decelle, J.; et al. The Protist Ribosomal Reference database (PR2): A catalog of unicellular eukaryote Small Sub-Unit rRNA sequences with curated taxonomy. *Nucleic Acids Res.* **2013**, *41*, D597–D604. [CrossRef]
30. Pruesse, E.; Peplies, J.; Glöckner, F.O. SINA: Accurate high-throughput multiple sequence alignment of ribosomal RNA genes. *Bioinformatics* **2012**, *28*, 1823–1829. [CrossRef]
31. Oksanen, J.; Simpson, G.L.; Blanchet, G.F.; Kindt, R.; Legendre, P.; Minchin, P.R.; O'Hara, R.B.; Solymos, P.; Stevens, M.H.H.; Szoecs, E.; et al. Vegan: Community Ecology Package. R Package Version 2.5–6. 2022. Available online: https://CRAN.R-project.org/package=vegan (accessed on 24 November 2022).

32. McMurdie, P.J.; Holmes, S. phyloseq: An R package for reproducible interactive analysis and graphics of microbiome census data. *PLoS ONE* **2013**, *8*, e61217. [CrossRef]
33. Kolde, R. _Pheatmap: Pretty Heatmaps_. R Package Version 1.0.12. 2019. Available online: https://CRAN.R-project.org/package=pheatmap (accessed on 16 May 2025).
34. Bodenhofer, U.; Kothmeier, A.; Hochreiter, S. APCluster: An R package for affinity propagation clustering. *Bioinformatics* **2011**, *27*, 2463–2464. [CrossRef]
35. Andersson, A.; Zhao, L.; Brugel, S.; Figueroa, D.; Huseby, S. Metabarcoding vs Microscopy: Comparison of methods to monitor phytoplankton communities. *ACS EST Water* **2023**, *3*, 2671–2680. [CrossRef]
36. Martens, N.; Russnak, V.; Woudhouse, J.; Grossart, H.-P.; Schaum, E. Metabarcoding reveals potentially mixotrophic flagellates and picophytoplankton as key groups of phytoplankton in the Elbe estuary. *Environ. Res.* **2024**, *252*, 119126. [CrossRef]
37. Bessudova, A.; Galachyants, Y.; Firsova, A.; Hilkhanova, D.; Nalimova, M.; Marchenkov, A.; Mikhailov, I.; Sakirko, M.; Likhoshway, Y. Changes in diversity of silica-scaled Chrysophytes during lake–river–reservoir transition (Baikal–Angara–Irkutsk Reservoir). *Life* **2023**, *13*, 2052. [CrossRef] [PubMed]
38. Kim, Y.-S.; Yun, H.-S.; Lee, J.-H.; Lee, K.-H.; Chpi, J.-S.; Won, D.H.; Kim, Y.J.; Kim, H.-S.; Yoon, H.-S. Comparison of Metabarcoding and Microscopy Methodologies to Analyze Diatom Communities in Five Estuaries Along the Southern Coast of the Korean Peninsula. *Microb. Ecol.* **2024**, *87*, 95. [CrossRef]
39. Urbach, E.K.; Vergin, L.; Young, L.; Morse, A.; Larson, G.L.; Giovannoni, S.J. Unusual bacterioplankton community structure in ultra-oligotrophic Crater Lake. *Limnol. Oceanogr.* **2001**, *46*, 557–572. [CrossRef]
40. Kaluzhnaya, O.V.; Itskovich, V.B.; McCormack, G.P. Phylogenetic diversity of bacteria associated with the endemic freshwater sponge *Lubomirskia baicalensis*. *World J. Microbiol. Biotechnol.* **2011**, *27*, 1955–1959. [CrossRef]
41. Clingenpeel, S.; Macur, R.E.; Kan, J.; Inskeep, W.P.; Lovalvo, D.; Varley, J.; Mathur, E.; Nealson, K.; Gorby, Y.; Jiang, H.; et al. Yellowstone Lake: High-energy geochemistry and rich bacterial diversity. *Environ. Microbiol.* **2011**, *13*, 2172–2185. [CrossRef]
42. Allgaier, M.; Grossart, H.P. Diversity and seasonal dynamics of Actinobacteria populations in four lakes in northeastern Germany. *Appl. Environ. Microbiol.* **2006**, *72*, 3489–3497. [CrossRef]
43. Warnecke, F.; Amann, R.; Pernthaler, J. Actinobacterial 16S rRNA genes from freshwater habitats cluster in four distinct lineages. *Environ. Microbiol.* **2004**, *6*, 242–253. [CrossRef]
44. Brinkmeyer, R.; Knittel, K.; Jürgens, J.; Weyland, H.; Amann, R.; Helmke, E. Diversity and structure of bacterial communities in Arctic versus Antarctic pack ice. *Appl. Environ. Microbiol.* **2003**, *69*, 6610–6619. [CrossRef]
45. Van den Wyngaert, S.; Salcher, M.M.; Pernthaler, J.; Zeder, M.; Posch, T. Quantitative dominance of seasonally persistent filamentous cyanobacteria (*Planktothrix rubescens*) in the microbial assemblages of a temperate lake. *Limnol. Oceanog.* **2011**, *56*, 97–109. [CrossRef]
46. Cheng, S.M.; Foght, J.M. Cultivation-independent and -dependent characterization of Bacteria resident beneath John Evans Glacier. *FEMS Microbiol. Ecol.* **2007**, *59*, 318–330. [CrossRef]
47. Crump, B.C.; Kling, G.W.; Bahr, M.; Hobbie, J.E. Bacterioplankton community shifts in an arctic lake correlate with seasonal changes in organic matter source. *Appl. Environ. Microbiol.* **2003**, *69*, 2253–2268. [CrossRef] [PubMed]
48. Newton, R.J.; Jones, S.E.; Helmus, M.R.; McMahon, K.D. Phylogenetic ecology of the freshwater Actinobacteria acI lineage. *Appl. Environ. Microbiol.* **2007**, *73*, 7169–7176. [CrossRef] [PubMed]
49. Xing, P.; Hahn, M.W.; Wu, Q.L. Low taxon richness of bacterioplankton in high-altitude lakes of the eastern tibetan plateau, with a predominance of *Bacteroidetes* and *Synechococcus* spp. *Appl. Environ. Microbiol.* **2009**, *75*, 7017–7025. [CrossRef]
50. Van Trappen, S.; Mergaert, J.; Van Eygen, S.; Dawyndt, P.; Cnockaert, M.C.; Swings, J. Diversity of 746 heterotrophic bacteria isolated from microbial mats from ten Antarctic lakes. *Syst. Appl. Microbiol.* **2002**, *25*, 603–610. [CrossRef]
51. Zwart, G.; Hiorns, W.D.; Methé, B.A.; van Agterveld, M.P.; Huismans, R.; Nold, S.C.; Zehr, J.P.; Laanbroek, H.J. Nearly identical 16S rRNA sequences recovered from lakes in North America and Europe indicate the existence of clades of globally distributed freshwater bacteria. *Syst. Appl. Microbiol.* **1998**, *21*, 546–556. [CrossRef]
52. Urbach, E.; Scanlan, D.J.; Distel, D.L.; Waterbury, J.B.; Chisholm, S.W. Rapid diversification of marine picophytoplankton with dissimilar light-harvesting structures inferred from sequences of *Prochlorococcus* and *Synechococcus* (Cyanobacteria). *J. Mol. Evol.* **1998**, *46*, 188–201. [CrossRef]
53. Wolf, A.; Wiese, J.; Jost, G.; Witzel, K.P. Wide geographic distribution of bacteriophages that lyse the same indigenous freshwater isolate (*Sphingomonas* sp. strain B18). *Appl. Environ. Microbiol.* **2003**, *69*, 2395–2398. [CrossRef]
54. Pernthaler, J.; Zöllner, E.; Warnecke, F.; Jürgens, K. Bloom of filamentous bacteria in a mesotrophic lake: Identity and potential controlling mechanism. *Appl. Environ. Microbiol.* **2004**, *70*, 6272–6281. [CrossRef]
55. Simpson, J.M.; Santo Domingo, J.W.; Reasoner, D.J. Assessment of equine fecal contamination: The search for alternative bacterial source-tracking targets. *FEMS Microbiol. Ecol.* **2004**, *47*, 65–75. [CrossRef] [PubMed]
56. Zwart, G.J.M.; Crump, B.C.; Agterveld, M.; Hagen, F.; Han, S.K. Typical freshwater bacteria: An analysis of available 16S rRNA gene sequences from plankton of lakes and rivers. *Aquat. Microb. Ecol.* **2002**, *28*, 141–155. [CrossRef]

57. Blunt, S.M.; Sackett, J.D.; Rosen, M.R.; Benotti, M.J.; Trenholm, R.A.; Vanderford, B.J.; Hedlund, B.P.; Moser, D.P. Association between degradation of pharmaceuticals and endocrine-disrupting compounds and microbial communities along a treated wastewater effluent gradient in Lake Mead Sci. *Total Environ.* **2017**, *622*, 1640–1648. [CrossRef] [PubMed]
58. Crosbie, N.D.; Pöckl, M.; Weisse, T. Dispersal and phylogenetic diversity of nonmarine picocyanobacteria, inferred from 16S rRNA gene and cpcBA-intergenic spacer sequence analyses. *Appl. Environ. Microbiol.* **2023**, *69*, 5716–5721. [CrossRef]
59. Simek, K.; Pernthaler, J.; Weinbauer, M.G.; Hornák, K.; Dolan, J.R.; Nedoma, J.; Masín, M.; Amann, R. Changes in bacterial community composition and dynamics and viral mortality rates associated with enhanced flagellate grazing in a mesoeutrophic reservoir. *Appl. Environ. Microbiol.* **2001**, *67*, 2723–2733. [CrossRef]
60. Stein, L.Y.; Jones, G.; Alexander, B.; Elmund, K.; Wright-Jones, C.; Nealson, K.H. Intriguing microbial diversity associated with metal-rich particles from a freshwater reservoir. *FEMS Microbiol. Ecol.* **2002**, *42*, 431–440. [CrossRef]
61. Tamaki, H.; Hanada, S.; Kamagata, Y.; Nakamura, K.; Nomura, N.; Nakano, K.; Matsumura, M. Flavobacterium limicola sp. nov., a psychrophilic, organic-polymer-degrading bacterium isolated from freshwater sediments. *Int. J. Syst. Evol. Microbiol.* **2003**, *53*, 519–526. [CrossRef]
62. Eder, W.; Schmidt, M.; Koch, M.; Garbe-Schönberg, D.; Huber, R. Prokaryotic phylogenetic diversity and corresponding geochemical data of the brine-seawater interface of the Shaban Deep, Red Sea. *Environ. Microbiol.* **2002**, *4*, 758–763. [CrossRef] [PubMed]
63. Zwart, G.; Huismans, R.; van Agterveld, M.P.; Van de Peer, Y.; De Rijk, P.; Eenhoorn, H.; Muyzer, G.; van Hannen, E.J.; Gons, H.J.; Laanbroek, H.J. Divergent members of the bacterial division Verrucomicrobiales in a temperate freshwater lake. *FEMS Microbiol. Ecol.* **1998**, *25*, 159–169. [CrossRef]
64. Balmonte, J.P.; Arnosti, C.; Underwood, S.; McKee, B.A.; Teske, A. Riverine Bacterial Communities Reveal Environmental Disturbance Signatures within the Betaproteobacteria and Verrucomicrobia. *Front. Microbiol.* **2016**, *7*, 1441. [CrossRef]
65. Reardon, C.L.; Cummings, D.E.; Petzke, L.M.; Kinsall, B.L.; Watson, D.B.; Peyton, B.M.; Geesey, G.G. Composition and diversity of microbial communities recovered from surrogate minerals incubated in an acidic uranium-contaminated aquifer. *Appl. Environ. Microbiol.* **2004**, *70*, 6037–6046. [CrossRef] [PubMed]
66. Jeon, C.O.; Park, W.; Padmanabhan, P.; DeRito, C.; Snape, J.R.; Madsen, E.L. Discovery of a bacterium, with distinctive dioxygenase, that is responsible for in situ biodegradation in contaminated sediment. *Proc. Natl. Acad. Sci. USA* **2003**, *100*, 13591–13596. [CrossRef] [PubMed]
67. Nelson, D.M.; Ohene-Adjei, S.; Hu, F.S.; Cann, I.K.; Mackie, R.I. Bacterial diversity and distribution in the holocene sediments of a northern temperate lake. *Microb. Ecol.* **2007**, *54*, 252–263. [CrossRef]
68. Matsubayashi, M.; Shimada, Y.; Li, Y.Y.; Harada, H.; Kubota, K. Phylogenetic diversity and in situ detection of eukaryotes in anaerobic sludge digesters. *PLoS ONE* **2017**, *12*, e0172888. [CrossRef]
69. Lefèvre, E.; Bardot, C.; Noël, C.; Carrias, J.F.; Viscogliosi, E.; Amblard, C.; Sime-Ngando, T. Unveiling fungal zooflagellates as members of freshwater picoeukaryotes: Evidence from a molecular diversity study in a deep meromictic lake. *Environ. Microbiol.* **2007**, *9*, 61–71. [CrossRef]
70. Medlin, L.K.; Kaczmarska, I. Evolution of the diatoms: V. Morphological and cytological support for the major clades and a taxonomic revision. *Phycologia* **2006**, *43*, 245–270. [CrossRef]
71. Edvardsen, B.; Eikrem, W.; Throndsen, J.; Sáez, A.G.; Probert, I.; Medlin, L.K. Ribosomal DNA phylogenies and a morphological revision provide the basis for a revised taxonomy of the Prymnesiales (Haptophyta). *Eur. J. Psychol.* **2011**, *46*, 202–228. [CrossRef]
72. Ki, J.S. Comparative molecular analysis of freshwater centric diatoms with particular emphasis on the nuclear ribosomal DNA of *Stephanodiscus* (Bacillariophyceae). *Algae* **2009**, *24*, 129–138. [CrossRef]
73. Mukherjee, I.; Hodoki, Y.; Nakano, S. Kinetoplastid flagellates overlooked by universal primers dominate in the oxygenated hypolimnion of Lake Biwa, Japan. *FEMS Microbiol. Ecol.* **2015**, *91*, fiv083. [CrossRef]
74. Rossi, A.; Boscaro, V.; Carducci, D.; Serra, V.; Modeo, L.; Verni, F.; Fokin, S.I.; Petroni, G. Ciliate communities and hidden biodiversity in freshwater biotopes of the Pistoia province (Tuscany, Italy). *Eur. J. Protistol.* **2016**, *53*, 11–19. [CrossRef]
75. Charvet, S.; Vincent, W.F.; Lovejoy, C. Chrysophytes and other protists in High Arctic lakes: Molecular gene surveys, pigment signatures and microscopy. *Polar Biol.* **2012**, *35*, 733–748. [CrossRef]
76. Gentekaki, E.; Lynn, D.H. Evidence for cryptic speciation in *Carchesium polypinum* Linnaeus, 1758 (Ciliophora: Peritrichia) inferred from mitochondrial, nuclear, and morphological markers. *J. Eukaryot. Microbiol.* **2010**, *57*, 508–519. [CrossRef]
77. Monchy, S.; Sanciu, G.; Jobard, M.; Rasconi, S.; Gerphagnon, M.; Chabé, M.; Cian, A.; Meloni, D.; Niquil, N.; Christaki, U.; et al. Exploring and quantifying fungal diversity in freshwater lake ecosystems using rDNA cloning/sequencing and SSU tag pyrosequencing. *Environ. Microbiol.* **2011**, *13*, 1433–1453. [CrossRef]
78. Dunthorn, M.; Stoeck, T.; Wolf, K.; Breiner, H.-W.; Foissner, W. Diversity and endemism of ciliates inhabiting Neotropical phytotelmata. *Syst. Biodivers.* **2012**, *10*, 195–205. [CrossRef]
79. Rad-Menéndez, C.; Stanley, M.; Green, D.H.; Cox, E.J.; Day, J.G. Exploring cryptic diversity in publicly available strains of the model diatom *Thalassiosira pseudonana* (Bacillariophyceae). *J. Mar. Biol. Assoc. United Kingd.* **2015**, *95*, 1081–1090. [CrossRef]

80. Andersen, R.A. Molecular systematics of the Chrysophyceae and Synurophyceae. In *Unravelling the Algae—The Past, Present, and Future of Algal Systematics, Systematics Association Special Volume*; Brodie, J., Lewis, J., Eds.; CRC Press: Boca Raton, FL, USA, 2007; pp. 285–313.
81. Luo, W.; Bock, C.; Li, H.R.; Padisak, J.; Krienitz, L. Molecular and microscopic diversity of planktonic eukaryotes in the oligotrophic Lake Stechlin (Germany). *Hydrobiologia* **2011**, *661*, 133–143. [CrossRef]
82. Oikonomou, A.; Katsiapi, M.; Karayanni, H.; Moustaka-Gouni, M.; Kormas, K.A. Plankton microorganisms coinciding with two consecutive mass fish kills in a newly reconstructed lake. *Sci. World J.* **2012**, *2012*, 504135. [CrossRef]
83. Choi, B.; Son, M.; Kim, J.I.; Shin, W. Taxonomy and phylogeny of the genus Cryptomonas (Cryptophyceae, Cryptophyta) from Korea. *Algae* **2013**, *28*, 307–330. [CrossRef]
84. Andersen, R.A.; Van de Peer, Y.; Potter, D.; Sexton, J.P.; Kawachi, M.; LaJeunesse, T. Phylogenetic analysis of the SSU rRNA from members of the Chrysophyceae. *Protist* **1999**, *150*, 71–84. [CrossRef]
85. Richards, T.A.; Vepritskiy, A.A.; Gouliamova, D.E.; Nierzwicki-Bauer, S.A. The molecular diversity of freshwater picoeukaryotes from an oligotrophic lake reveals diverse, distinctive and globally dispersed lineages. *Environ Microbiol.* **2005**, *7*, 1413–1425. [CrossRef]
86. Kahn, P.; Herfort, L.; Peterson, T.D.; Zuber, P. Discovery of a Katablepharis sp. in the Columbia River estuary that is abundant during the spring and bears a unique large ribosomal subunit sequence element. *MicrobiologyOpen* **2014**, *3*, 764–776. [CrossRef] [PubMed]
87. Weisse, T.; Strüder-Kypke, M.C.; Berger, H.; Foissner, W. Genetic, morphological, and ecological diversity of spatially separated clones of *Meseres corlissi* Petz & Foissner, 1992 (Ciliophora, Spirotrichea). *J. Eukaryot Microbiol.* **2008**, *55*, 257–270. [CrossRef]
88. Tarbe, A.; Stenuite, S.; Balagué, V.; Sinyinza, D.; Descy, J.; Massana, R. Molecular characterisation of the small-eukaryote community in a tropical Great Lake (Lake Tanganyika, East Africa). *Aquat. Microb. Ecol.* **2011**, *62*, 177–190. [CrossRef]
89. Gao, F.; Li, J.; Song, W.; Xu, D.; Warren, A.; Yi, Z.; Gao, S. Multi-gene-based phylogenetic analysis of oligotrich ciliates with emphasis on two dominant groups: Cyrtostrombidiids and strombidiids (Protozoa, Ciliophora). *Mol. Phylogenet. Evol.* **2016**, *105*, 241–250. [CrossRef]
90. Karpov, S.A.; Tcvetkova, V.S.; Mamkaeva, M.A.; Torruella, G.; Timpano, H.; Moreira, D.; Mamanazarova, K.S.; López-García, P. Morphological and Genetic Diversity of Opisthosporidia: New Aphelid *Paraphelidium tribonemae* gen. et sp. Nov. *J. Eukaryot. Microbiol.* **2017**, *64*, 204–212. [CrossRef] [PubMed]
91. Lefranc, M.; Thénot, A.; Lepère, C.; Debroas, D. Genetic diversity of small eukaryotes in lakes differing by their trophic status. *Appl. Environ. Microbiol.* **2005**, *71*, 5935–5942. [CrossRef]
92. Tuji, A.; Mohri, Y.; Ki, J.-S.; Jung, S.W.; Julius, M.L. Phylogeny of *Praestephanos* gen. nov. (Thalassiosirales, Bacillariophyceae) based on *Stephanodiscus suzukii*, and related freshwater thalassiosiroid diatoms. *Plankton Benthos Res.* **2014**, *9*, 132–140. [CrossRef]
93. Kaczmarska, I.; Beaton, M.; Benoit, A.C.; Medlin, L.K. Molecular phylogeny of selected members of the order Thalassiosirales (Bacillariophyta) and evolution of the fultoportula. *J. Phycol.* **2006**, *42*, 121–138. [CrossRef]
94. Yamamoto, M.; Nozaki, H.; Kawano, S. Evolutionary relationships among multiple modes of cell division in the genus Nannochloris (Chlorophyta) revealed by genome size, actin gene multiplicity, and phylogeny. *J. Phycol.* **2001**, *37*, 106–120. [CrossRef]
95. Pröschold, T.; Darienko, T.; Silva, P.C.; Reisser, W.; Krienitz, L. The systematics of Zoochlorella revisited employing an integrative approach. *Environ. Microbiol.* **2011**, *13*, 350–364. [CrossRef]
96. Bhattacharya, D.; Medlin, L.; Wainright, P.O.; Ariztia, E.V.; Bibeau, C.; Stickel, S.K.; Sogin, M.L. Algae containing chlorophylls a + c are paraphyletic: Molecular evolutionary analysis of the CHROMOPHYTA. *Evolution* **1993**, *47*, 1801–1817. [CrossRef]
97. Jeong, M.; Kim, J.I.; Nam, S.W.; Shin, W. Molecular Phylogeny and Taxonomy of the Genus Spumella (Chrysophyceae) Based on Morphological and Molecular Evidence. *Front. Plant Sci.* **2021**, *26*, 758067. [CrossRef]
98. Song, W.; Xu, D.; Zhang, Q.; Liu, W.; Warren, A.; Song, W. Taxonomy and phylogeny of two poorly studied genera of marine oligotrich ciliates including descriptions of two new species: *Cyrtostrombidium paraboreale* sp. N. and *Apostrombidium orientale* sp. N. (Ciliophora: Spirotrichea). *Eur. J. Protistol.* **2019**, *70*, 1–16. [CrossRef] [PubMed]
99. Bachy, C.; Gómez, F.; López-García, P.; Dolan, J.R.; Moreira, D. Molecular phylogeny of tintinnid ciliates (Tintinnida, Ciliophora). *Protist* **2012**, *163*, 873–887. [CrossRef]
100. Nakai, R.; Abe, T.; Baba, T.; Imura, S.; Kagoshima, H.; Kanda, H.; Kohara, Y.; Koi, A.; Niki, H.; Yanagihara, K.; et al. Eukaryotic phylotypes in aquatic moss pillars inhabiting a freshwater lake in East Antarctica, based on 18S rRNA gene analysis. *Polar Biol.* **2012**, *35*, 1495–1504. [CrossRef]
101. Newbold, L.K.; Oliver, A.E.; Booth, T.; Tiwari, B.; Desantis, T.; Maguire, M.; Andersen, G.; van der Gast, C.J.; Whiteley, A.S. The response of marine picoplankton to ocean acidification. *Environ. Microbiol.* **2012**, *14*, 2293–2307. [CrossRef]
102. Medlin, L.; Jung, I.; Bahulikar, R.; Mendgen, K.; Kroth, P.; Kooistra, W.H.C.F. Evolution of the diatoms. VI. Assessment of the new genera in the araphids using molecular data. *Nova Hedwig.* **2008**, *133*, 81–100.
103. Vd'ačný, P.; Bourland, W.A.; Orsi, W.; Epstein, S.S.; Foissner, W. Phylogeny and classification of the Litostomatea (Protista, Ciliophora), with emphasis on free-living taxa and the 18S rRNA gene. *Mol. Phylogenet Evol.* **2011**, *59*, 510–522. [CrossRef]

104. Chen, M.; Chen, F.; Yu, Y.; Ji, J.; Kong, F. Genetic diversity of eukaryotic microorganisms in Lake Taihu, a large shallow subtropical lake in china. *Microb. Ecol.* **2008**, *56*, 572–583. [CrossRef]
105. Boenigk, J.; Pfandl, K.; Stadler, P.; Chatzinotas, A. High diversity of the 'Spumella-like' flagellates: An investigation based on the SSU rRNA gene sequences of isolates from habitats located in six different geographic regions. *Environ. Microbiol.* **2005**, *7*, 685–697. [CrossRef]
106. Atkins, M.S.; Teske, A.P.; Anderson, O.R. A survey of flagellate diversity at four deep-sea hydrothermal vents in the Eastern Pacific Ocean using structural and molecular approaches. *J. Eukaryot. Microbiol.* **2000**, *47*, 400–411. [CrossRef] [PubMed]

Disclaimer/Publisher's Note: The statements, opinions and data contained in all publications are solely those of the individual author(s) and contributor(s) and not of MDPI and/or the editor(s). MDPI and/or the editor(s) disclaim responsibility for any injury to people or property resulting from any ideas, methods, instructions or products referred to in the content.